Journal of Alloys and Compounds 509 (2011) 5320–5325

Contents lists available at ScienceDirect

Journal of Alloys and Compounds

journal homepage: www.elsevier.com/locate/jallcom

Preparation and structural properties of Lu_2O_3:Eu^{3+} submicrometer spherical phosphors

Yulia V. Yermolayeva*, Alexander V. Tolmachev, Maria V. Dobrotvorskaya, Oleh M. Vovk

Scientific and Technological Corporation, Institute for Single Crystals, NAS of Ukraine, 61001, 60 Lenin Ave, Kharkov, Ukraine

ARTICLE INFO

Article history:
Received 12 May 2010
Received in revised form 1 February 2011
Accepted 5 February 2011
Available online 17 February 2011

Keywords:
Rare earth alloys and compounds
Chemical synthesis
Precipitation
Crystal structure
X-ray diffraction

ABSTRACT

Monodisperse non-agglomerated Lu_2O_3:Eu^{3+} submicrometer spheres were obtained by the homogeneous precipitation technique with subsequent annealing for spheres crystallization. The morphological and structural parameters of the Lu_2O_3:Eu^{3+} crystalline spheres prepared were investigated by the electron microscopy methods, thermal analysis (TG-DTA), X-ray diffractometry (XRD), X-ray photoelectron (XPS) and FT-IR spectroscopy. The influence of the annealing temperature on the morphology and sphericity was shown. Eu^{3+}-doped lutetium oxide spheres were characterized by effective luminescence under X-ray excitation in the λ = 575–725 nm range corresponding to $^5D_0 \rightarrow {}^7F_J$ transitions (J = 0–4) of Eu^{3+} ions. It was shown that the X-ray luminescence efficiency of the Lu_2O_3:Eu^{3+} spherical phosphors prepared strongly depend on annealing temperature and dopant concentration.

1. Introduction

Nowadays, monodisperse spherical particles of the varied compositions are widely studied due to the prospective application both in practical and fundamental aspects. Colloidal suspensions of the nano- and submicrospheres (SiO_2, TiO_2, polymer etc. [1–3]) are playing an increasingly important role as model systems to study a variety of phenomena in condensed matter physics in real space, such as nucleation, growth mechanisms and rheology aspects.

Moreover spherical particles show ability to self-organization in ordered photonic crystals (PhCs), a promising optical materials due to the possibility Bragg-reflect the light with the wavelength defined by the spheres diameter [4,5]. Highly efficient light-emitting materials for display technologies (cathode ray tubes, plasma display panels, and field emission displays) can be achieved by the placing of the luminescent component inside the PhC, it can be realized by using of the phosphor spheres as structural units for such photonic crystals preparing. Thus, its stimulate active progress in development and study of the inorganic luminescent spherical nano- and submicron particles of the mixed compositions (rare-earth doped SiO_2, Y_2O_3:Eu^{3+}, $(Y_{1-x}Gd_x)_2O_3$:Eu^{3+}, etc. [6–8]) or with core–shell structure [9,10].

To extend phosphors to high resolution applications, fine phosphor particles with ideal spherical morphology, controllable diameters, narrow size distribution and homogeneous composition as well as required surface properties for the self-assembling would be highly desirable. A variety of methods have been successfully applied to the preparation of the spherical phosphors, including sol–gel and hydrothermal technology, precipitation route, combustion and spray pyrolysis methods [8,11–15]. Among these methods, urea-based homogeneous precipitation (UBHP) technique is widely used for the synthesis of the inorganic particles with the highly controllable sizes and well-defined morphologies by taking advantages of the slow decomposition of urea at the temperatures above 80 °C. The in situ decomposition of urea releases of the precipitating ligands (OH^- and CO_3^{2-}) slowly and homogeneously into the reaction system, avoiding localized distribution of the reactants and thus making it possible to exercise control over nucleation and growth. The UBHP technique was employed to precipitate amorphous colloidal spheres of the mixed Y/Gd, Y/Eu, Gd/Eu basic carbonates (precursor) with subsequent annealing for the polycrystalline rare-earth oxides resultant particles obtaining [7,12,14].

The luminescence parameters of the phosphor particles are strongly depend on its morphology, surface area, crystallite sizes, which is defined by the synthesis conditions, reagents concentration, etc. The morphology dependent luminescence properties of Y_2O_3:Eu^{3+} phosphors prepared were analyzed earlier [8,16,17]. Thus, it was concluded that the spherical morphology is good for improving the emission intensity as well as that particles with

* Corresponding author.
E-mail address: yermolayeva@isc.kharkov.ua (Y.V. Yermolayeva).

0925-8388/$ – see front matter © 2011 Elsevier B.V. All rights reserved.
doi:10.1016/j.jallcom.2011.02.022

a smaller surface area showed higher photoluminescence intensity. The luminescence intensities were also found to be strongly dependent on crystallites size for Y_2O_3:Eu^{3+} and Gd_2O_3:Eu^{3+} polycrystalline particles [8,18].

Lutetium oxide (Lu_2O_3) doped with trivalent europium (Eu^{3+}) ions is a structural analog of effective commercial Y_2O_3:Eu^{3+} red phosphor, and belongs to cubic structure, space group Ia3. It is reported earlier that lutetium is more favorable cation than yttrium for lanthanide dopant emission [19]. Moreover, Lu_2O_3:Eu^{3+} is one of the most perspective material for X-ray detection and imaging due to high effective atomic number $Z_{eff.} = 67$ and its extremely high density ($\rho = 9.4\ g/cm^3$) in comparison with Y_2O_3 ($\rho = 4{,}8\ g/cm^3$) and Gd_2O_3 ($\rho = 7{,}6\ g/cm^3$). Lu_2O_3:Eu^{3+} was obtained and studied in different forms such as powders (including nanocrystalline), sol–gel films and transparent ceramics [20,21]. Preparation, morphology and structure features of the Lu_2O_3:Eu^{3+} spherical particles has not been properly described yet [22]. Lu_2O_3:Eu^{3+} in the form of the nanoshells on SiO_2 spheres was prepared by us earlier for the creation of the spherical and size controlled phosphors [9]. However, the principal drawback of the luminescent nanoshells is lower luminescence efficiency comparatively with bulk materials due to the surface quenching processes through the decrease of the volume/surface ratio of the phosphor layer. That is why, the bare Lu_2O_3:Eu^{3+} spherical particles were chosen as investigation object in the present study.

In this work, we report a systematic experimental study regarding the preparing of the Lu_2O_3:Eu^{3+} spheres by UBHP method and their characterization and also the influence of the annealing temperature on the structure and morphology of the Lu_2O_3:Eu^{3+} phosphors.

2. Experimental

The Lu_2O_3:Eu^{3+} spheres were obtained by the UBHP technique. Europium content was ranged from 1 to 10 at.% with respect to lutetium. Firstly, high-purity lutetium oxide (Lu_2O_3, 99.99%) and europium oxide (Eu_2O_3, 99.99%) powders were dissolved in nitric acid to form $Lu(NO_3)_3$ and $Eu(NO_3)_3$ solutions. Synthesis procedure was carried out in water solution of $Lu(NO_3)_3$ (2×10^{-3} mol/L), $Eu(NO_3)_3$ and urea ($(NH_2)_2CO$) as a precipitant. The molar ratio [Lu^{3+}]/[urea] was 0.002 for preparing the precursor particles with the diameter about 130 nm [22]. The reactive mixture was heated at 85 ± 1 °C to decompose the urea and stirred during 5 h. The resulting precursor was separated by centrifugation, washed several times with ethanol and water, and dried at 60–80 °C to prevent "soft" agglomerates formation [22]. Finally, the precursor obtained was exposed by heating in air in 500–1200 °C temperature range for 2 h to produce the final crystalline spherical particles.

The morphology of the samples obtained was studied by means of scanning electron microscopy (SEM) using a JSM-6390 LV (JEOL, Japan) and a transmission electron microscopy (TEM) using a EM-125 (Selmi, Ukraine). The X-ray diffraction (XRD) of the powder samples was examined on a DRON-3M diffractometer using CoK_α radiation ($\lambda = 1.79021$ Å). The average sizes of Lu_2O_3:Eu^{3+} crystallites were found from the broadening of the [2 2 2], [4 0 0] and [4 4 0] diffraction lines of the X-ray patterns according to Scherrer's formula: $D = K\lambda/(\beta\cos\Theta)$, where λ is the X-ray wavelength, β is the full-width at the half-maximum of the diffraction line located at Θ angle. The thermal analysis (TG-DTA) was conducted using a MOM Q-1500 derivatograph in air within a temperature interval 20–1000 °C at heating rate of 10 °C/min. Fourier transform infrared spectroscopy (FT-IR) spectra of the samples were measured on a FT-IR spectrometer SPECTRUM ONE (Perkin-Elmer) with the KBr pellet technique. The surface composition of the particles prepared was studied with X-ray photoelectron spectroscopy (XPS) with a spectrometer XSAM-800 Kratos using MgK_α – radiation ($h\gamma = 1253.6$ eV). X-ray luminescence spectra of the samples were obtained using SDL-2 (LOMO, Russia) automated complex. X-ray luminescence was excited by REIS-E X-ray source (Cu-anticathode, deceleration radiation with the energy $E \sim 30$ keV), operating at $U = 30$ kV and $I = 50$ mkA.

3. Results and discussion

3.1. Crystallization, structure and temperature effects

The urea-precipitated and dried at 60 °C precursor spheres of the europium-doped lutetium basic carbonate ($Lu(OH)CO_3$:$Eu{\cdot}H_2O$) composition were amorphous to X-rays. Scanning electron microscopy (SEM) was used for the morphology analysis in a large scale of the freshly prepared spheres (Fig. 1a). It is clearly seen that $Lu(OH)CO_3$:$Eu{\cdot}H_2O$ particles have perfect spherical shape, uniform size distribution and keep they individuality without agglomeration. Energy dispersive X-ray spectrum of precursor particles includes the peaks attributed to Lu, O and C elements presence (Fig. 1b). Statistical analysis of the particles size distribution carried out using SEM data points to a narrow size distribution for the obtained samples (Fig. 1c).

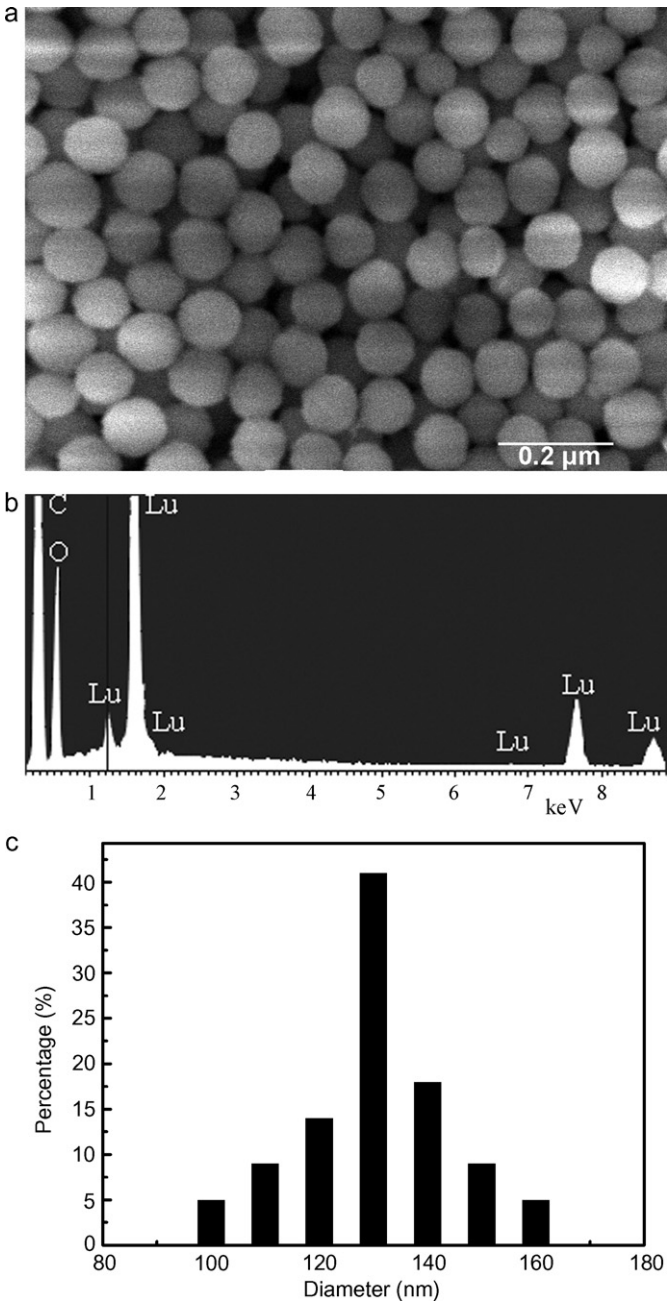

Fig. 1. SEM image (a), EDS analysis (b) and histogram for the size distribution (c) of the $Lu(OH)CO_3$:$Eu{\cdot}H_2O$ precursor particles.

The thermal analysis was used for the studying of the precursor particles decomposition and crystallization process. TG-DTA curves of the precursor powders dried at 60 °C are given in Fig. 2. DTA shows one endothermic peak at about 190 °C corresponds to release of hydration water, a shallow peak in the region of 320–530 °C, which is related with precursor decomposition and exothermic

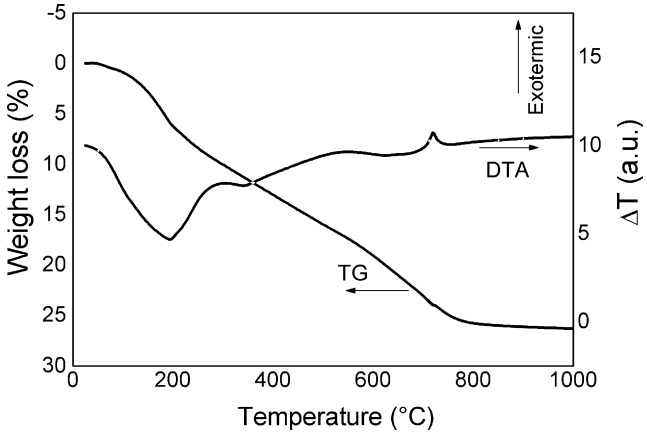

Fig. 2. TG-DTA curves of the precursor particles dried at 60 °C.

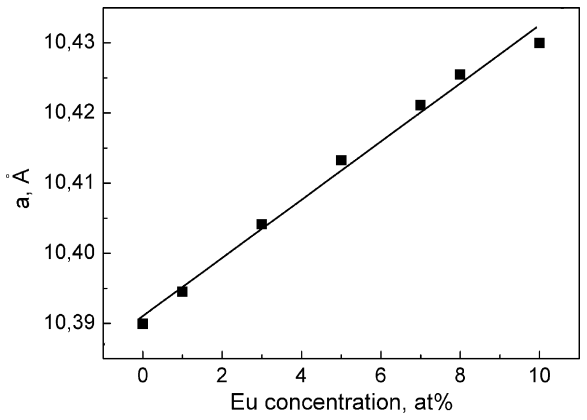

Fig. 4. Lattice parameter (a, Å) as a function of Eu^{3+} concentration.

peak at 720 °C is due to the lutetium oxide crystallization. The TG curve shows two steps weight loss up to 850 °C. Thus, it is possible to suggest the following mechanism of the thermal decomposition of $Lu(OH)CO_3{:}Eu{\cdot}H_2O$ into $Lu_2O_3{:}Eu$:

$$Lu(OH)CO_3 : Eu \cdot H_2O \overset{60-245\,^\circ C}{\longrightarrow} \underset{(7\,wt\%)}{Lu(OH)CO_3 : Eu} \overset{245-550\,^\circ C}{\longrightarrow}$$

$$\times \underset{(10-18\,wt\%)}{\text{intermediate phases}} \overset{550-850\,^\circ C}{\longrightarrow} \underset{(26\,wt\%)}{Lu_2O_3 : Eu},$$

where the possible intermediate phases are $Lu_2(CO_3)_3{:}Eu$, $Lu_2O(CO_3)_2{:}Eu$, $Lu_2O_2CO_3{:}Eu$ [23,24]. The experimental total weight loss is about 26% and in a good agreement with the theoretical one.

X-ray diffraction patterns of the resultant particles after heat treatment are presented in Fig. 3. The particles prepared at the temperatures up to crystallization point are amorphous, however the material heated up to 600 °C show very broad strongly overlapping XRD peaks which indicate that the spherical powders possess some crystalline areas. The intensive narrow diffraction peaks correspond to the (2 1 1), (2 2 2), (4 0 0), (4 1 1), (3 3 2), (4 3 1), (4 4 0), (6 1 1) and (6 2 2) planes are registered in the patterns of the samples annealed at temperatures above 800 °C proving that crystallization process is already complete. These peaks are belonging to crystalline cubic Lu_2O_3 structure (JCPDS card 12-0728). With increasing of the annealing temperature the diffraction patterns become progressively narrower, which corresponds to an increase of the crystallite size and improvement of the material crystallinity. No impurity peaks were observed, indicating that the spherical powders prepared are pure in both chemistry and crystalline phase.

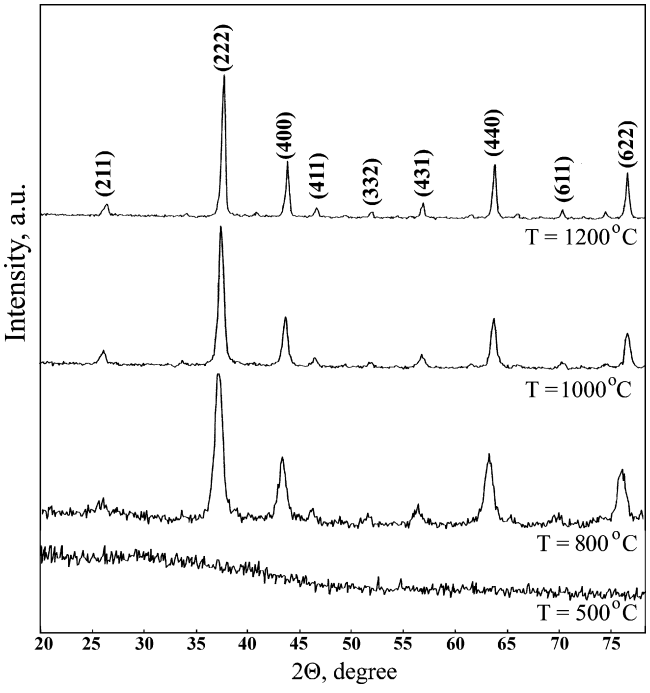

Fig. 3. X-ray diffraction patterns of the spherical particles annealed at the specified temperatures for 2 h.

The lattice parameter calculated for the undoped Lu_2O_3 particles ($a = 10.390 \pm 0.006$ Å) coincides well with the theoretical value. Incorporation of the Eu^{3+} dopant in the Lu_2O_3 cubic structure leads to the increase of lattice parameter value due to the isomorphous substitution of Lu^{3+} (ionic radius 0.84 Å) by the bigger Eu^{3+} ion (0.96 Å) and can be registered by the shifting of the diffraction line towards smaller angles as the concentration of Eu^{3+} increases. The linear dependence of the lattice parameter on europium content observed in the particles is shown in Fig. 4, which testify about homogeneous $Lu_2O_3{:}Eu^{3+}$ substitutional solid solution formation in the given concentration range. The europium concentration in the samples was controlled by means of inductively coupled plasma atomic emission spectroscopy (ICP-AES).

The effect of the annealing temperature on the spheres diameters and morphology was studied by means of transmission electron microscopy (TEM). The results showed that the thermal decomposition of precursor particles accompanying about 20% decrease of the particles average diameter. The dependence of the particles diameter versus annealing temperature is shown in Fig. 5a (curve 1) is in a good agreement with the TG curve and have two characteristic plots: (1) up to 400 °C – intensive particles diameter decrease due to lutetium basic carbonate decomposition; (2) 400–800 °C – less intensive decrease of the particles diameter, which occur during intermediate phases decomposition and crystallization. As expected the average diameter was not changed above 800 °C after the crystallization process was finished. The $Lu_2O_3{:}Eu^{3+}$ spheres have the polycrystalline structure. The average crystallites sizes (Scherrer size) of the spherical powders annealed at specified temperatures were calculated from XRD patterns using the Scherrer equation (Fig. 5a, curve 2). The size of crystallites is clearly seen to rise with the increase of annealing temperature. Thus, it can be supposed that the intensive crystallites size growth during thermal treatment collides with the spherical shape stability of the particles. The TEM images show the morphology evolution of the $Lu_2O_3{:}Eu^{3+}$ particles (Fig. 5b). It is clearly seen that tendency towards agglomeration of the spheres increases at the temperature above 900 °C because of the sticking between particles. Moreover,

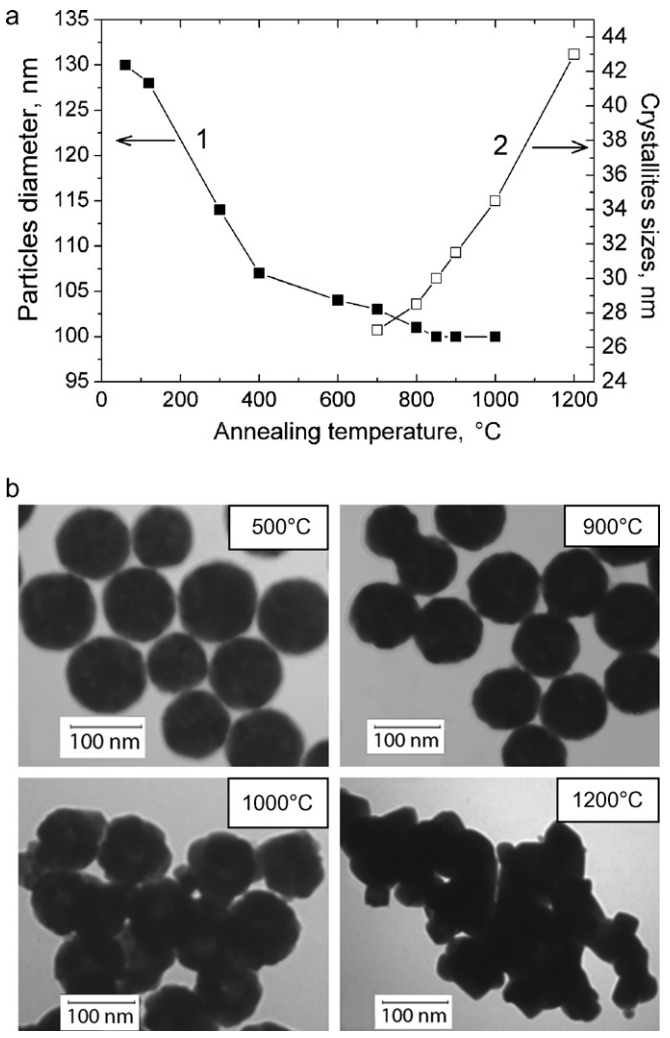

Fig. 5. Particles diameter (1) and Scherrer's crystallites sizes (2) of Lu_2O_3:Eu^{3+} spheres depending on annealing temperature (a) and TEM images of the resultant particles (b).

at the temperature above 1000 °C the crystalline spheres destroyed probably because of the increasing of the stresses inside the particle as a result of the re-crystallization processes.

3.2. FT-IR spectroscopy

FT-IR spectra recorded for the spherical particles samples annealed at the different temperatures are shown in Fig. 6. FT-IR spectrum for precursor particles has the absorption band near 3435 cm^{-1}, which is assigned to stretching vibration of O–H bonds. Two intensive bands at 1530 cm^{-1} and 1403 cm^{-1} are observed in the spectrum, which are concerned with the asymmetric stretch of C–O in CO_3^{2-} groups. The absorption bands at 1092 cm^{-1} and 840 cm^{-1} are assigned as symmetric stretch of C–O band and deformation vibration of C–O in CO_3^{2-} groups, respectively [24]. These absorption bands indicate the presence of carbonate groups (CO_3^{2-}) in the lutetium basic carbonate precursor. The C–O group's bands are disappeared after the 700 °C annealing, which connected with the precursor decomposition and CO_2 removing. Appearance of Lu–O (491 cm^{-1} and 575 cm^{-1}) bands testifies about crystalline lutetium oxide formation. It is necessary to notice that only the heating at 1200 °C let getting rid of residual OH-impurities, which strongly influences on the luminescence intensity.

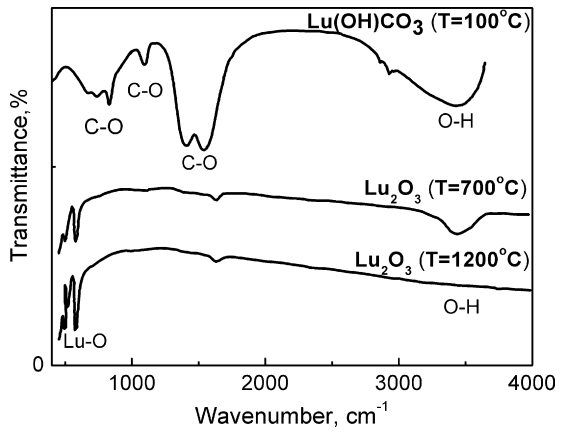

Fig. 6. FT-IR spectra of the spherical particles annealed at specified temperatures.

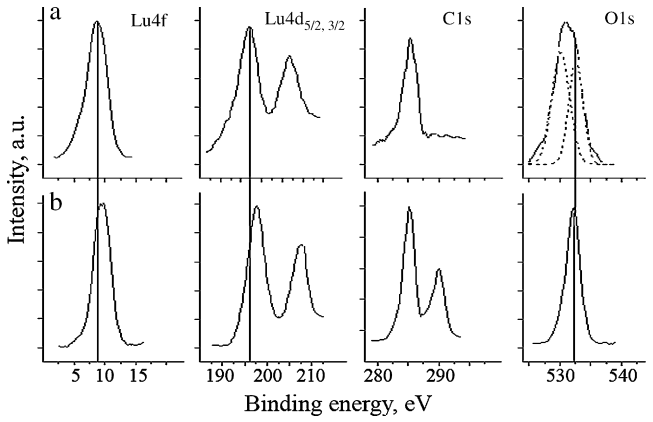

Fig. 7. Normalized X-ray photoelectron spectra of Lu4f, Lu4d, C1s, O1s-levels of the spherical particles samples: (a) – precursor spheres, (b) – Lu_2O_3 spheres (annealed at 900 °C).

3.3. XPS analysis

The normalized XPS spectra of Lu4f, Lu4d, C1s and O1s-levels of the dried precursor $Lu(OH)CO_3 \cdot H_2O$ spheres as well as Lu_2O_3 annealed spheres at 900 °C are presented in Fig. 7. The lines position in the Lu4f (E_b = 9.2 eV), Lu4d (E_b = 197.2 eV) and O1 s (E_b = 532.3 eV) spectra (Fig. 7a) of the precursor samples before annealing corresponding well with the literature data for the lutetium hydroxide [25]. In the XPS core level C1s spectrum of the precursors spheres (Fig. 7a) the two lines are observed with the binding energy

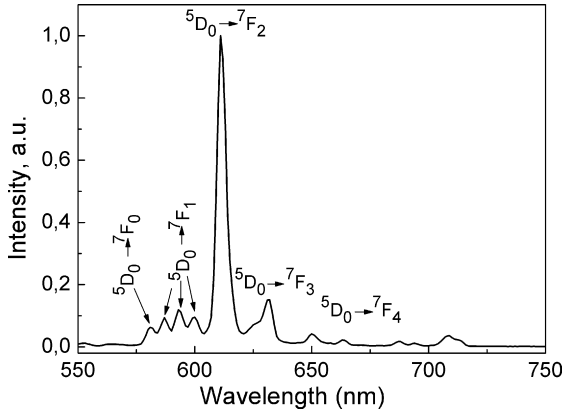

Fig. 8. Room-temperature X-ray-exited luminescence spectrum of Lu_2O_3:Eu^{3+} (5 at.%) spherical particles.

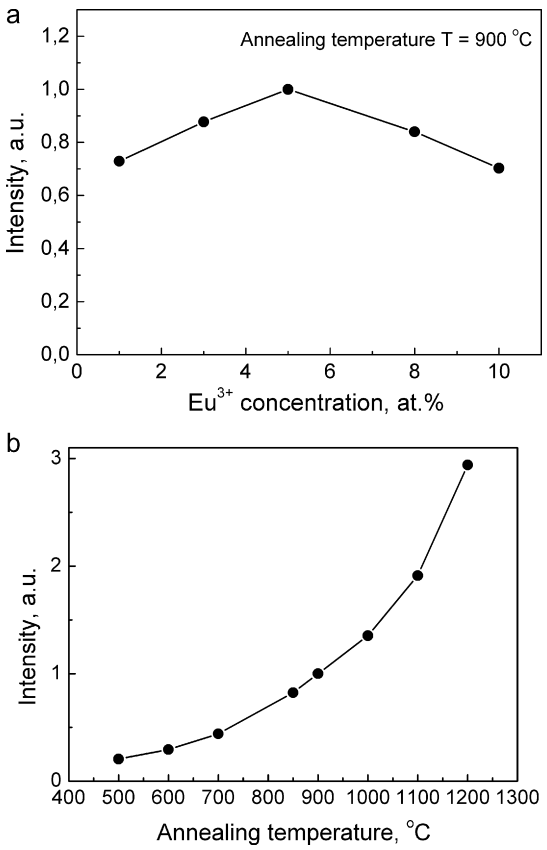

Fig. 9. The X-ray luminescence integral intensity of Lu_2O_3:Eu^{3+} spherical particles depend on annealing temperature (a) and europium ions concentration (b).

285.0 eV and 290.0 eV, which are fit with hydrocarbon compounds absorbed on the sample surface and C–O band in CO_3^{2-} groups, respectively. Thus, it was proved based on FT-IR and XPS methods that the $Lu(OH)CO_3{\cdot}H_2O$ precursor was urea-precipitated during spherical particles synthesis. The following changes are observed in the spectra after samples annealing (Fig. 7b): (1) the line at 290.0 eV in the C1s – spectrum is not observed and (2) the Lu4f and Lu4d lines shift for 1 eV to lower binding energies and also (3) the line with the binding energy 530.0 eV in the O1s spectrum is appeared. Such binding energies values are typical for crystalline lutetium oxides [26], which along with FT-IR data testify about lutetium oxide Lu_2O_3 phase formation during samples annealing.

3.4. X-ray luminescence

Fig. 8 presents the normalized luminescence spectrum under X-ray excitation of the Lu_2O_3:Eu^{3+} spheres. Luminescence spectrum consists of a group of lines in the $\lambda = 575–725$ nm spectral region corresponding to $^5D_0 \rightarrow {}^7F_J$ transitions ($J = 0–4$) of Eu^{3+} ions and conform well to emission of the Eu^{3+} ions in the Lu_2O_3 host lattice [27]. The $^5D_0 \rightarrow {}^7F_2$ electric dipole transitions with the maximum at $\lambda = 611$ nm are dominant, and the emission falls within the spectral sensitivity range of CCD camera. In the cubic Lu_2O_3 lattice two different sites are available for Eu^{3+} ions with C_2 and C_{3i} (S_6) symmetry. The Eu^{3+} ions in the C_2 noncentrosymmetric site demonstrate forced 4*f*–4*f* electric dipole transitions, while the Eu^{3+} ions in the symmetrical site of C_{3i} (S_6) are characterized only by magnetic dipole transitions with significantly lower intensity. Thus, the X-ray luminescence spectrum of the Lu_2O_3:Eu^{3+} presented in Fig. 8 corresponds to the superposition of emission of the Eu^{3+} ions occupying in Lu_2O_3 host different crystallographic positions. The high luminescence intensity of the Lu_2O_3:Eu^{3+} sphere samples under X-ray excitation evidences the presence of an efficient channel of the energy transfer from matrix to the Eu^{3+} emission centers according to a recombination mechanism [28].

The influence of the annealing temperature as well as europium concentration on the integral X-ray luminescence intensity of the Lu_2O_3:Eu^{3+} spheres was studied in detail. By varying of the Eu^{3+} content in Lu_2O_3 host, we determined the compositions with the highest X-ray-exited emission intensity. Fig. 9a shows the dependence of the radioluminescence intensity on the Eu^{3+} ions concentration in the Lu_2O_3:Eu^{3+} spheres. The maximum of X-ray luminescence intensity was observed for europium ions concentration of about 5 at.%. The further increase of the Eu^{3+} ions content results in the decrease of the luminescence yield due to the concentration quenching effect.

Fig. 9b shows the luminescence intensity of the Lu_2O_3:Eu^{3+} (5 at.%) spheres depending on the annealing temperature. It is clearly seen that with the rising of the annealing temperature the luminescence intensity increases. First of all, this fact can be related to the rising of the crystallites sizes (Fig. 5a) and as a result improvement of the particles crystallinity. Furthermore, luminescence increasing is probably caused by the removal of quenching impurities, particularly hydroxyl-groups (OH) [29], which was observed according to FT-IR results (Fig. 6). However, along with significant enhancement of the spherical particles luminescence with the increasing of annealing temperature the loss of sphericity take place and the agglomeration processes become more effective that limits the practical application of the particles annealed at temperatures above 1000 °C.

4. Conclusions

Uniform-sized submicrometer spherical Lu_2O_3:Eu^{3+} phosphors have been obtained by the urea-based homogeneous precipitation with subsequent annealing at the temperatures ranging from 500 °C to 1200 °C for the precursor decomposition and crystallization. Combined analysis of TG-DTA, FT-IR and XPS characterizations reveals that the precursor has a lutetium basic carbonate composition and its thermal decomposition process includes the removal of hydration water, OH^- and CO_3^{2-} ions during annealing. It was shown that the annealing temperature strongly influences on the structure, morphology and composition of the spherical Lu_2O_3:Eu^{3+} phosphors obtained. Lu_2O_3:Eu^{3+} cubic phase is found to crystallize complete at 800 °C and heat treatment above 1000 °C results in deformation of the spherical shape of the particles and also initiates the processes of sintering and agglomeration. However the improvement of the particles crystallinity and removing residual quenching centers (OH) at the high temperatures leads to increase the X-ray luminescence efficiency of Lu_2O_3:Eu^{3+} phosphors. The phosphor spheres developed in this work are attractive as building blocks for scintillation films for X-ray imaging and also for new types of photonic structures.

Acknowledgments

The authors are grateful to Dr V.F. Tkachenko and Dr R.P. Yavetskiy for the help in testing of the experimental samples by XRD method and X-ray luminescence measurements.

References

[1] A. van Blaaderen, J.V. Geest, A. Vrij, J. Colloid Interface Sci. 154 (1992) 481.
[2] S. Eiden-Assmann, J. Widoniak, G. Maret, Chem. Mater. 16 (2004) 6.
[3] D.L. Green, J.S. Lin, Y.-F. Lam, M.Z. Hu, D.W. Schaefer, M.T. Harris, J. Colloid Interface Sci. 266 (2003) 346.
[4] F. Juillerat, P. Bowen, H. Hofmann, Langmuir 22 (2006) 2249.

[5] L. Pallavidino, D. Santamaria Razo, F. Geobaldo, A. Balestreri, D. Bajoni, M. Galli, L.C. Andreani, C. Ricciardi, E. Celasco, M. Quaglio, F. Giorgis, J. Non-Cryst. Solids 352 (2006) 1425.
[6] M.J.A. de Dood, B. Berkhout, C.M. van Kats, A. Polman, A. van Blaaderen, Chem. Mater. 14 (2002) 2849.
[7] J.G. Li, X.D. Li, X.D. Sun, T. Ikegami, T. Ishigaki, Chem. Mater. 20 (2008) 2274.
[8] W.-N. Wang, W. Widiyastuti, T. Ogi, I.W. Lenggoro, K. Okuyama, Chem. Mater. 19 (2007) 1723.
[9] Yu.V. Yermolayeva, A.V. Tolmachev, T.I. Korshikova, R.P. Yavetskiy, M.V. Dobrotvorskaya, N.I. Danylenko, D.S. Sofronov, Nanotechnology 20 (2009) 325601.
[10] Yu.V. Yermolayeva, Yu.N. Savin, A.V. Tolmachev, Solid State Phenom. 151 (2009) 264.
[11] M.A. Flores-Gonzalez, C. Louis, R. Bazzi, G. Ledoux, K. Lebbou, S. Roux, P. Perriat, O. Tillement, Appl. Phys. A 81 (2005) 1385.
[12] Y.C. Kang, I.W. Lenggoro, S.B. Park, K. Okuyama, J. Phys. Chem. Solids 60 (1999) 1855.
[13] L. Sun, C. Qian, C. Liao, X. Wang, C. Yan, Solid State Commun. 119 (2001) 393.
[14] H. Giesche, E. Matijevic, J. Mater. Res. 9 (1994) 436.
[15] H.S. Yoo, H.S. Jang, W.B. Im, J.H. Kang, D.Y. Jeon, J. Mater. Res. 22 (2007) 2017.
[16] L.S. Wang, Y.H. Zhou, Z.W. Quan, J. Lin, Mater. Lett. 59 (2005) 1130.
[17] K.Y. Jung, C.H. Lee, Y.C. Kang, Mater. Lett. 59 (2005) 2451.
[18] W.N. Wang, W. Widiyastuti, I.W. Lenggoro, T.O. Kim, K. Okuyama, J. Electrochem. Soc. 154 (2007) J121.
[19] J.C. Boyer, F. Vetrone, J.A. Capobianco, A. Speghini, M. Bettinelli, J. Phys. Chem. B 108 (2004) 20137.
[20] A. Garcia-Murillo, C.L. Luyer, C. Dujardin, T. Martin, C. Garapon, C. Pedrini, J. Mugnier, NIM A 486 (2002) 181.
[21] V.V. Nagarkar, S.R. Miller, S.V. Tipnis, A. Lempicki, C. Brecher, H. Lingertat, NIM B 213 (2004) 250.
[22] N.A. Dulina, Y.V. Yermolayeva, A.V. Tolmachev, Z.P. Sergienko, O.M. Vovk, E.A. Vovk, N.A. Matveevskaya, P.V. Mateychenko, J. Eur. Ceram. Soc. 30 (2010) 1717.
[23] B. Aiken, W.P. Hsu, E. Matijevik, J. Am. Ceram. Soc. 71 (1988) 845.
[24] Q. Chen, Y. Shi, L. An, S. Wang, J. Chen, J. Shi, J. Eur. Ceram. Soc. 27 (2007) 191.
[25] A. Zenkevich, Yu. Lebedinskii, S. Spiga, C. Wiemer, G. Scarel, M. Fanciulli, Microelectron. Eng. 84 (2007) 2263.
[26] Y.A. Teterin, Y.A. Teterin, Russ. Chem. Rev. 71 (2002) 347.
[27] E. Zych, J. Phys.: Condens. Matter 14 (2002) 5637.
[28] E. Zych, J. Trojan-Piegza, Chem. Mater. 18 (2006) 2194.
[29] E. Zych, J. Trojan-Piegza, L. Kepinski, Sens. Actuators B 109 (2005) 112.